

adder are summarised in Table 1. The proposed adder has a better power efficiency. It can also operate at a speed comparable to the other adders. In terms of area, the proposed adder is the most effective among all the studied adders. The transistor count of the proposed adder is 18 comparing to 48 for a DPL adder, 28 for a CPL adder and 28 for both the SRPL and SRPL2 adder. Besides, it does not require complementary input signals as in other adders. Thus, the overall circuit size is reduced further.

**Table 1:** Comparison of adder performance

| Adder    | Power dissipation at 5V/mW | Power dissipation at 3V/mW | Delay at 5V/ns | Delay at 3V/ns |
|----------|----------------------------|----------------------------|----------------|----------------|
| Proposed | 0.512                      | 0.252                      | 0.896          | 1.353          |
| CPL      | 1.707                      | 0.708                      | 0.668          | 1.123          |
| DPL      | 1.611                      | 0.813                      | 0.538          | 0.888          |
| SRPL     | 3.831                      | 1.934                      | 0.831          | 1.173          |
| SRPL2    | 3.887                      | 2.005                      | 0.667          | 1.021          |

**Conclusion:** This Letter has described a low power and compact VLSI circuit for adder implementation. It is suitable for designs where power and size are the major design constraints. Comparison showed that the proposed adder consumes less power than the other high speed CMOS based circuits including complementary pass transistor logic, dual pass transistor logic, and swing restored pass-transistor logic. The reduction in power consumption is the result of fewer number of transistors used in the design. Simulation results showed that the proposed adder consumes three times less energy than the CPL and DPL adder, and seven times less energy than the SRPL and SRPL2 adder, at both 3 and 5V supply. Our simulation result also showed that the speed of the proposed adder is comparable to the others. Hence, the design of the circuit does not compromise the circuit performance with power consumption.

© IEE 1997

3 February 1997

Electronics Letters Online No: 19970464

A. Wu and C.K. Ng (EDA Centre, Department of Electronic Engineering, City University of Hong Kong, Tat Chee Avenue, Kowloon, Hong Kong)

## References

- MATASUZAWA, A.: 'Low-voltage and low-power circuit design for mixed analogue/digital systems in portable equipment', *IEEE J. Solid-State Circuits*, 1994, **29**, (4), pp. 470-480
- KO, U., BALSARA, P.T., and LEE, W.: 'Low-power design techniques for high-performance CMOS adders', *IEEE Trans. Very Large Scale Integr. Syst.*, 1995, **3**, (2), pp. 327-333
- YANO, K., YAMANAKA, T., NISHIDA, T., SAITO, M., SHIMOHIGASHI, K., and SHIMIZU, A.: 'A 3.8-ns CMOS 16x16-bit multiplier using complementary pass-transistor logic', *IEEE J. Solid-State Circuits*, 1990, **25**, pp. 388-395
- SUZUKI, M., SHINBO, K., YAMANAKA, T., SHIMIZU, A., SASAKI, K., and NAKAGOME, Y.: 'A 1.5-ns 32b CMOS ALU in dual pass-transistor logic', *IEEE J. Solid-State Circuits*, 1993, **28**, pp. 1145-1151
- PARAMESWAR, A., HARA, H., and SAKURAI, T.: 'A high-speed, low-power, swing restored pass-transistor logic based multiply and accumulate circuit for multimedia applications'. Proc. IEEE 1994 CICC, pp. 278-281
- NJOLSTAD, T., and AAS, E.J.: 'Power consumption and performance of low-voltage bit-serial adders'. Proc. IEEE 1996 ISCAS, pp. 45-48
- WU, A.: 'High performance pipelined multiplier with fast carry-save adder'. 2nd NASA SERC Symp. VLSI Design, 1990

## Optical switching in two-mode semiconductor lasers via gain or loss modulation

Ching-Fuh Lin, Pei-Cheng Ku, Yu-Li Hsueh and Chaur-Shiuann Juang

*Indexing terms:* Semiconductor junction lasers, Optical switches

The authors demonstrate an optical switching mechanism based on two-mode lasers in which bistability does not exist. Both theoretical analysis and experiment show that a small amount of gain or loss modulation is sufficient to cause switching between two oscillating modes.

Optical computing and optical communication require fast optical modulation and switching. Several methods have been used for this purpose. Direct intensity modulation on the laser diode provides the advantage of simplicity, but it suffers the inherent limitation caused by relaxation oscillation. The use of a lithium niobate (LiNbO<sub>3</sub>) Mach-Zehnder modulator as an external modulator is an alternative candidate, but it usually requires a high drive voltage ( $V_{\pi} \geq 5$ ) [1]. The use of an MQW electroabsorption modulator has recently attracted much attention [2]. However, it involves sophisticated material growth techniques. In this Letter, we propose optical switching based on the two-mode laser via gain or loss modulation. The switching between the two oscillation modes could be achieved via a small amount of modulation. Similar switching used to be demonstrated in two-mode bistability [3], in which lasing is toggled between two competing cavity modes [4-6]. However switching using bistability requires that the controlled variable is changed beyond the range for hysteresis. For the two-mode laser that does not have bistability, switching between the two oscillation modes can be even more easily achieved because no hysteresis regime needs to be passed during switching.

The idea of optical switching based on the two-mode laser is very simple and can be easily understood using two-mode competition theory [7] although it can also be derived from the multi-mode rate equations. A slight extension from two-mode competition theory [7] can quickly lead to the condition for the simultaneously stable oscillation of both modes:

$$\frac{g_2 - l_2 C_{12}}{g_2 S_2} < \frac{g_1 - l_1}{g_1} < \frac{g_2 - l_2 S_1}{g_2 C_{21}} \quad (1)$$

where  $S$  and  $C$  are the self-saturation and cross-saturation coefficients, respectively;  $g$  is the unsaturated gain and  $l$  is the cavity loss of each mode.

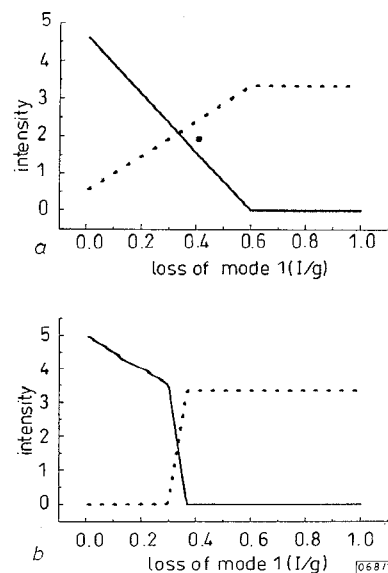


**Fig. 1** Illustrations of mode competition via loss modulation for  $g_1 = g_2 = 1$ ,  $l_2 = 0$ , and  $C_{21}/S_1 = C_{12}/S_2 = 0.6$  and  $0.95$

a 0.6  
b 0.95  
— mode 1  
..... mode 2

Switching between mode 1 and 2 should occur if gain or loss varies beyond the region given by eqn. 1. The switching range also depends on the values of the ratios,  $S_1/C_{21}$  and  $C_{12}/S_2$ . Fig. 1 shows the numerical calculation of the switching situation for different ratios of  $S_1/C_{21}$  and  $C_{12}/S_2$ . Because this laser does not exhibit bistability, there is no hysteresis. For two-mode lasers with a very strong gain competition, the cross-saturation product  $C_{12}C_{21}$  is very close to the self-saturation product  $S_1S_2$ . Therefore, switching between these two modes can be achieved via only a very small amount of loss or gain modulation, as shown in Fig. 1b.

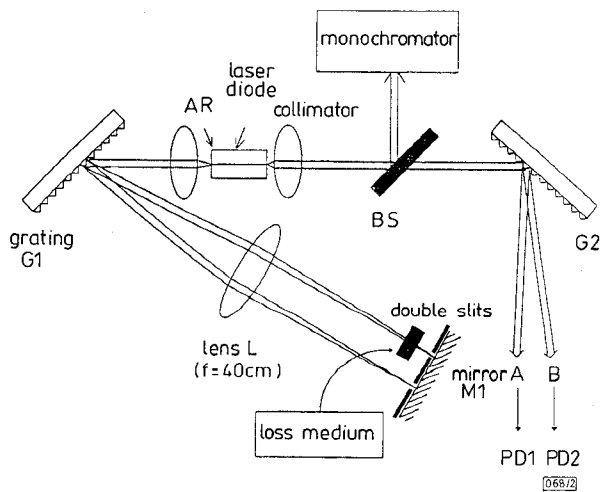


Fig. 2 Schematic diagram of optical switching in two-mode semiconductor laser in experiment

PD1, PD2: photodetector  
G1, G2: grating  
BS: beam splitter  
Loss medium is cover glass mounted on rotary base

An experimental demonstration of optical switching between two oscillation wavelengths via loss modulation was carried out. A schematic diagram of the experimental setup is shown in Fig. 2. A standard ridge-waveguide laser diode is used in the setup. It has a  $4 \mu\text{m}$  wide ridge-waveguide structure fabricated on an AlGaAs/GaAs substrate. The light emitted from the AR-coated facet ( $R \approx 4.6 \times 10^{-3}$ ) is collimated by an objective. A reflected-type grating telescope configuration [8] is used in the external cavity. As the mirror is placed at a focal distance from the lens, as shown in Fig. 2, different wavelengths will return into the same gain region, although they travel along different paths in the external cavity. V-shaped double slits are placed in front of the mirror to select two wavelengths for switching experiments.

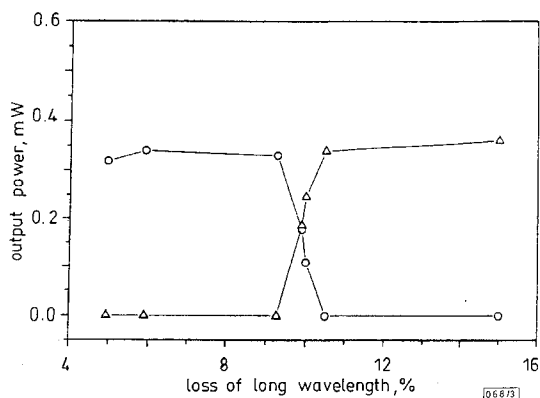


Fig. 3 Measured intensities of mode 1 (long wavelength) and mode 2 (short wavelength) against insertion loss of mode 1

○ long wavelength  
△ short wavelength

One or several cover glasses mounted on a rotary base are inserted in the path of mode 1, as shown in Fig. 2, so the loss of mode 1 can be modulated by rotating the cover glass or inserting more cover glasses. The Fabry-Perot effect of the cover glass makes the loss vary with rotating angle, but not monotonically

with the incident angle. Conversely, because the cover glass is very thin, it has little influence on the optical path and is experimentally found to cause a negligible wavelength shift of mode 1, regardless of the rotating angle in the experiment. Initially, the loss of cover glass is adjusted to have a loss of 10% and the slit is moved horizontally [8] to have two modes oscillating with almost equal intensity. Then switching between the two modes is observed as the cover glass is rotated. Fig. 3 shows the intensity of each mode against calibrated loss. It is found that  $< 1\%$  of loss variation is sufficient to cause switching. Switching could also be possibly achieved by an electronically or optically controlled manner, e.g. via direct modulation on the monolithically integrated absorber or injection of the third-mode light, which will be further explored in the future.

Such switching is different from the conventional wavelength tuning from one mode to another in a continuous way [9], where only one mode has a large gain and the others are suppressed with significant losses. In our work, both modes have significant gains and the switching is mainly caused by the cross-saturation effect. Therefore, the use of a single-stripe laser diode is essential because the two modes could then have a good overlap in the gain region to cause a strong gain competition. The farfield emission patterns for the oscillation of either mode (with one slit blocked) and the simultaneous oscillation of both modes were measured using a CCD camera. The nearly identical farfield emission patterns indicate that the two modes should overlap significantly in the gain region and so each mode has almost the same saturation effect on itself and the other. Therefore,  $S_1/C_{21}$  and  $C_{12}/S_2$  approach one and switching between these two modes can be achieved via a very small amount of loss. In addition, the cross-saturation characteristics of the two modes are mainly governed by the intraband relaxation of the carriers. As a result, the switching speed is primarily limited by the intraband relaxation lifetime, instead of the spontaneous-emission lifetime, and so is expected to be fast.

In conclusion, optical switching based on two-mode lasers is demonstrated theoretically and experimentally. Theoretical analysis shows that switching between the two oscillating modes can be achieved by a small amount of gain or loss modulation. The experiment demonstrates that  $< \pm 1\%$  of loss modulation is sufficient to cause optical switching between two lasing wavelengths in such a two-mode semiconductor laser. The efficient switching capability is due to the strong gain competition of the lasing modes.

*Acknowledgment:* This work is supported in part by the National Science Council, Taipei, Taiwan, Republic of China, under contract NSC85-2112-M-002-018. The authors would like to acknowledge Bor-Lin Lee for his technical assistance.

© IEE 1997

27 January 1997

Electronics Letters Online No: 19970435

Ching-Fuh Lin, Pei-Cheng Ku, Yu-Li Hsueh and Chaur-Shiuann Juang (Graduate Institute of Electro-Optical Engineering and Department of Electrical Engineering, National Taiwan University, Taipei, Taiwan, Republic of China)

## References

- LOI, K.K., SAKAMOTO, I., MEI, X.B., TU, C.W., and CHANG, W.S.C.: 'High-efficiency 1.3mm InAsP-GaInP MQW electroabsorption waveguide modulators for microwave fiber-optic links', *IEEE Photonics Technol. Lett.*, 1996, **8**, pp. 626-628
- SHEN, L., WIEDER, H.H., and CHANG, W.S.C.: 'Electroabsorption modulation at 1.3mm on GaAs substrates using a step-graded low temperature grown InAlAs buffer', *IEEE Photonics Technol. Lett.*, 1996, **8**, pp. 352-354
- KAWAGUCHI, H.: 'Bistability in laser diodes' (Artech House, 1994)
- KLEHR, A., MULLER, R., VOSS, M., and BARWOLFF, A.: 'Gigahertz switching behavior of polarization-bistable InGaAsP/InP lasers under high-frequency current modulation', *Appl. Phys. Lett.*, 1994, **64**, pp. 830-832
- UENOHARA, H., KAWAMURA, Y., IWAMURA, H., NONAKA, K., TSUDA, H., and KUROKAWA, T.: 'Side-light-injection MQW bistable laser using saturable absorption and gain quenching', *Electron. Lett.*, 1992, **28**, pp. 1973-1975

- 6 JOHNSON, J.E., and TANG, C.L.: 'Optical flip-flop based on two-mode intensity bistability in a cross-coupled bistable laser diode', *Appl. Phys. Lett.*, 1993, **63**, pp. 3273–3275
- 7 SIEGMAN, A.E.: 'Lasers' (University Science Books, 1986)
- 8 LIN, : 'Selected multi-wavelength oscillation of a semiconductor laser in an external cavity'. Paper TuEB, 1995 Semiconductor Lasers: Advanced Devices and Applications, 1995, (Keystone, Colorado)
- 9 SCHREMER, A.T., and TANG, C.L.: 'External-cavity semiconductor laser with 1000GHz continuous piezoelectric tuning range', *IEEE Photonics Technol. Lett.*, 1990, **2**, pp. 3–5

## Bandstop series stubs for coplanar waveguide on GaAs

T.M. Weller, K.J. Herrick and L.P.B. Katehi

*Indexing terms: Coplanar waveguides, Gallium arsenide*

The authors present measured characteristics of several types of coplanar waveguide series tuning stubs printed on gallium arsenide. These stubs exhibit a bandstop response that is useful for microwave and millimetre-wave filtering applications. Herein, the primary emphasis is placed on compact stub geometries which have resonant lengths as small as 0.1 guide wavelengths.

**Introduction:** Coplanar waveguide series tuning stubs are very useful and versatile components for microwave and millimetre-wave (mm-wave) applications [1–3]. Typically, the series configuration is implemented by routing the slots of the CPW line through the centre conductor, thereby deforming the centre conductor into multiple fingers. This laterally compact geometry enhances field confinement and results in less radiation loss than that of stubs which are printed in the ground planes [4].

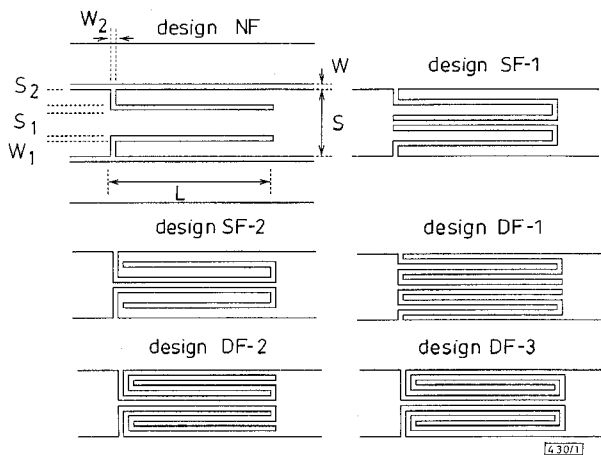


**Fig. 1** Conventional and compact CPW series stub configurations

In each case,  $S_1$  refers to centre finger width and  $S_2$  refers to width of all outer fingers  
Coplanar ground planes are only shown for design NF

This Letter focuses on the use of short-end stub geometries in which the series stub is folded back upon itself to reduce size. The benchmark for the results is a configuration in which one pair of coupled slots is defined within the CPW centre conductor; this will be referred to as the conventional, or non-folded approach, and is shown in Fig. 1. More efficient use of circuit area can be achieved by using the single- and double-folded designs, which are also shown in Fig. 1. The primary objective of this work was to investigate the relative merits of the folded stub designs on the basis of size, depth of the bandstop notch, and insertion loss.

The circuits were fabricated on 350 $\mu\text{m}$ -thick, high resistivity GaAs using the design specifications given in Table 1. In each case, the total ground plane width is  $4(S + 2W)$  and the gold lines were electroplated to a thickness of 2.7 $\mu\text{m}$ .

**Bandstop series stubs:** To illustrate typical stub performance, the scattering parameters of a conventional, non-folded design are shown in Fig. 2. For this example the stub length is  $L = 1900\mu\text{m}$  and the bandstop resonance occurs at 15GHz ( $f_0$ ), corresponding to a resonant length of  $\sim 0.25$  guide wavelengths. Each stub geometry considered herein exhibits a response which is similar to that of the non-folded stub up to the bandpass resonance at  $\sim 2f_0$ ; as an example, the scattering parameters of a 720 $\mu\text{m}$  long type DF-1 stub are also included in Fig. 2. In addition to resonant length, two other figures of merit that will be used for comparison are the notch depth at  $f_0$  and the insertion loss at  $0.5f_0$ , which are  $-16$  and  $-0.9\text{dB}$ , respectively, for the non-folded design in Fig. 2.

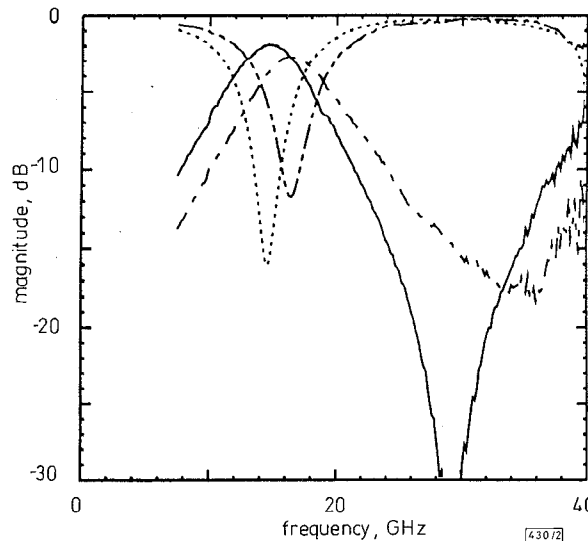


**Fig. 2** Measured scattering parameters for type NF-1 ( $L = 1900\mu\text{m}$ ) and type DF-1 ( $L = 720\mu\text{m}$ ) short-end stubs

— NF-1  $S_{11}$   
 ..... NF-1  $S_{21}$   
 - - - - DF-1  $S_{11}$   
 - - - - DF-1  $S_{21}$

The electrical length of each short-end stub geometry at the first band-stop resonance is shown in Fig. 3. Here, the physical stub length is normalised to  $\lambda_0$ , which is the free-space wavelength at  $f_0$ . The non-folded stubs resonate at  $\sim 0.092\lambda_0$ , while single-folded SF-2 and double-folded DF-3 configurations resonate at  $0.052\lambda_0$  and  $0.036\lambda_0$ , respectively.

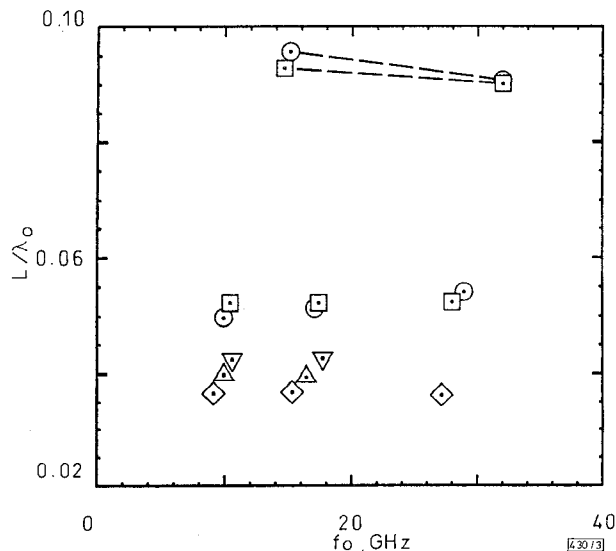


**Fig. 3** Normalised short-end stub length against resonant frequency

$\lambda_0$ : free-space wavelength at  $f_0$   
 ○— NF-1  
 □— NF-2  
 ○ SF-1  
 □ SF-2  
 △ DF-1  
 ▽ DF-2  
 ◇ DF-3